

Detection of the magnetar SGR J1745–2900 up to 291 GHz with evidence of polarized millimetre emission

P. Torne,^{1*} G. Desvignes,¹ R. P. Eatough,¹ R. Karuppusamy,¹ G. Paubert,³
M. Kramer,^{1,2} I. Cognard,^{4,5} D. J. Champion,¹ and L. G. Spitler¹

¹Max-Planck-Institut für Radioastronomie, Auf dem Hügel 69, D-53121, Bonn, Germany

²Jodrell Bank Centre for Astrophysics, School of Physics and Astronomy, The University of Manchester, Manchester M13 9PL, UK

³Instituto de Radioastronomía Milimétrica, Avda. Divina Pastora 7, Núcleo Central, 18012, Granada, Spain

⁴Laboratoire de Physique et Chimie de l’Environnement et de l’Espace CNRS-Université d’Orléans, F-45071, Orléans, France

⁵Station de radioastronomie de Nançay, Observatoire de Paris, CNRS/INSU, F-18330, Nançay, France

Accepted 2016 October 21. Received 2016 October 17; in original form 2016 June 27

ABSTRACT

In Torne et al. (2015), we showed detections of SGR J1745–2900 up to 225 GHz (1.33 mm); at that time the highest radio frequency detection of pulsar emission. In this work, we present the results of new observations of the same magnetar with detections up to 291 GHz (1.03 mm), together with evidence of linear polarization in its millimetre emission. SGR J1745–2900 continues to show variability and is, on average, a factor ~ 4 brighter in the millimetre band than in our observations of July 2014. The new measured spectrum is slightly inverted, with $\langle\alpha\rangle = +0.4 \pm 0.2$ (for $S_\nu \propto \nu^\alpha$). However, the spectrum does not seem to be well described by a single power law, which might be due to the intrinsic variability of the source, or perhaps a turn-up somewhere between 8.35 and 87 GHz. These results may help us to improve our still incomplete model of pulsar emission and, in addition, they further support the search for and study of pulsars located at the Galactic Centre using millimetre wavelengths.

Key words: stars: neutron – pulsars: general – pulsars: individual: SGR J1745–2900 – stars: magnetars – radiation mechanisms: non-thermal

1 INTRODUCTION

Magnetar is the term used to refer to neutron stars whose high-energy luminosities can exceed their spin-down luminosity. These objects typically show large inferred magnetic fields ($B \gtrsim 10^{13}$ G), and it is widely accepted that they require energy from magnetic field decay to power their emission, particularly at high energies (Duncan & Thompson 1992; Thompson & Duncan 1995, 1996). The magnetars make up a small family within the pulsar population, with only 23 objects confirmed (see The Magnetar Catalog¹, Olausen & Kaspi 2014). They are typically detected through their high-energy emission, but four of them have also shown radio pulsations (Camilo et al. 2006, 2007b; Levin et al. 2010; Eatough et al. 2013).

SGR J1745–2900 is one of the radio emitting magnetars, and its location at the Galactic Centre, close to Sgr A* (Bower et al. 2015), makes it a particularly interesting object. Studying the propagation effects of its emission can

provide valuable information about the environment close to the supermassive black hole at the centre of the Galaxy and along the line-of-sight (e.g. Eatough et al. 2013; Shannon & Johnston 2013; Bower et al. 2014; Spitler et al. 2014).

The radio emission of magnetars is similar to that of the normal population of pulsars, but shows some remarkable differences. For example, their flux density, spectral index, pulse profile shape, and polarization properties have been seen to vary on short and long time scales (Camilo et al. 2006, 2007b; Kramer et al. 2007; Lazaridis et al. 2008; Levin et al. 2012; Lynch et al. 2015). Such variability is inconsistent in most cases with propagation effects, and it is considered intrinsic to the source.

Another peculiar characteristic of magnetar radio emission is the tendency to be spectrally flat, and SGR J1745–2900 is no exception (Torne et al. 2015). This is interesting because pulsars, being typically steep spectrum sources (with mean spectral index $\langle\alpha\rangle = -1.8$, Maron et al. 2000), are difficult to detect at radio frequencies above a few gigahertz. In fact, only seven normal pulsars have been detected above 30 GHz to date (Wiełebinski et al. 1993; Kramer et al. 1997; Morris et al. 1997; Löhmer et al. 2008).

* E-mail: ptorne@mpeifr-bonn.mpg.de

¹ www.physics.mcgill.ca/~pulsar/magnetar/main.html

SGR J1745–2900 held the record, prior to this work, with detections up to 225 GHz (Torne et al. 2015), followed by XTE J1810–197 up to 144 GHz (Camilo et al. 2007c).

The study of the characteristics of pulsar radio emission at high frequencies can help to elucidate how the emission from neutron stars is produced; a problem that remains unresolved since the discovery of pulsars almost 50 years ago (see e.g. Hankins et al. 2009; Melrose & Yuen 2016). For instance, some models predict a possible turn-up in the spectrum at sufficiently high frequencies, due to incoherent emission becoming dominant (Michel 1978, 1982). Observational works have reported an excess of flux density for some of the pulsars studied at millimetre wavelengths (Wielebinski et al. 1993; Kramer et al. 1996, 1997), giving credibility to those models. However, the sample of pulsar observations at high radio frequencies is small. More observations are needed to study better the behaviour of the high frequency emission, and to check for turn-ups or other unpredicted effects.

Because of its high luminosity and flat spectrum (Torne et al. 2015), SGR J1745–2900 is a superb source to be observed at very high radio frequencies, especially at the short millimetre regime where there is almost no information about pulsar radiation. This work presents the results from a multifrequency campaign for SGR J1745–2900 carried out at frequencies between 2.54 and 291 GHz (wavelengths between 11.8 cm and 1.03 mm) aiming to obtain further information about its emission properties and providing additional constraints for pulsar emission models.

2 OBSERVATIONS AND DATA ANALYSIS

The millimetre observations were made with the 30-m radio telescope of the Institut de Radioastronomie Millimétrique (IRAM) during 2015 March 4–9. The receiver used was the Eight MIXer Receiver (EMIR, Carter et al. 2012). EMIR delivers four separated, tunable frequency bands between ~73 and 350 GHz (4 and 0.8 mm) in dual linear polarization². During the six days of observations different set-ups were used, mainly depending on weather, covering between 87 and 291 GHz. The Broad-Band-Continuum (BBC) backend recorded the four bands tuned in EMIR with ~6 GHz of bandwidth each (~24 GHz in total), no frequency resolution (i.e. total power mode), with a sampling time of 1 ms. After several upgrades, the intermediate frequency (IF) range of all EMIR mixers is 4 to 12 GHz which is directly fed to the BBC power detectors. However, there is a significant slope in the passband, which favours the lower frequencies, and we have therefore taken 6 GHz (instead of 8 GHz) as the properly weighted effective IF bandwidth. The sky frequency values corresponding to the centre of the 4–12 GHz IF range of the used EMIR mixers are 87, 101, 138, 154, 209, 225, 275, and 291 GHz.

In addition to the observations with the IRAM 30-m, we observed simultaneously at certain epochs with the Effelsberg 100-m radio telescope and with the Nançay 94-m equivalent radio telescope. At Effelsberg, two different observing frequencies were used, centred at 4.85 and 8.35 GHz.

At Nançay, the central frequency was 2.54 GHz. The set-up, data reduction and calibration of the Effelsberg and Nançay data were identical to those already described in Torne et al. (2015). Table 1 summarizes the observations.

At IRAM, each observing session consisted typically of 45-min scans on SGR J1745–2900 with interspersed “hot-cold-sky” calibration measurements. Additionally, a few scans on planets were used to verify the absolute flux density calibration, obtained following the methodology in Kramer (1997), and applying elevation and frequency-dependent gain corrections (Peñalver 2012).

Typical “switching techniques” used in millimetre observations to subtract the atmospheric contribution are not adequate for pulsar observations. Thus, the time series at millimetre wavelengths required careful processing to enhance the detections of the magnetar. This is because of a significant amount of red noise present in the data, mostly due to variations in the atmospheric water vapour content during the observations. Such effect can be particularly bad for observations of SGR J1745–2900 due to its long period and the low elevation at which the IRAM 30-m sees the Galactic Centre (elevation < 25 deg), which translates into a considerable airmass³. The data showed also periodic interference, the most prominent being at 1 and 50 Hz and some of their harmonics, most likely related to the cryogenerator and the mains power.

The cleaning process was as follows. First, the time series was Fourier transformed and prominent interference was removed by zapping a few spectral bins around each peak at 1, 2, 50, 55, 60, 100 and 200 Hz. After an inverse Fourier transform, the resulting time series was filtered by a running mean with a window length of 10 s. To prevent the filtering from degrading the magnetar pulses, we used an ephemeris from a timing model to predict the times of arrival of the pulses at the observatory, and protected a window of 0.81 s (approximately the pulse width) around each time-of-arrival. This was achieved by extrapolating 3.75 s of the running mean vector from each side of the protection window by using a third-degree polynomial. For the two highest observing frequencies, 275 and 291 GHz, we extrapolated a shorter block of running mean vector of only 0.05 s to each side, using a linear interpolation, which gave better results. Once we had a modified time series with the content of the protected windows substituted by the extrapolated data, we apply a running mean on this new time series that is then subtracted from the original one. This method is effective at cleaning the pulse, while avoiding the artefacts caused by the running mean. Next, we removed some negative spikes that occasionally appear in the time series by substituting all negative values of the time series larger than -6σ with the median of the time series. A final step was to apply a second running mean filter with a smaller window of 0.4 s, again protecting the pulse window, to remove short-term variations.

The result of the cleaning process is a high signal-to-noise folded profile with nearly flat off-pulse baseline. The mean flux density (i.e. the integrated profile intensity averaged over the full period) is calculated by summing the area

² For more information on the EMIR frequency combinations, see <http://www.iram.es/IRAMES/mainWiki/EmirforAstronomers>

³ Airmass refers to the amount of Earth’s atmosphere that a celestial signal passes through along the line of sight.

under the pulse and dividing by the number of bins in the profile. Flux density errors are estimated from the off-pulse noise and also include the uncertainties in the absolute calibration factors, estimated to 10, 20 and 30 per cent for the 3, 2 and 1 mm bands, respectively.

3 RESULTS AND DISCUSSION

3.1 Detections, flux density and spectrum

SGR J1745–2900 was detected at all frequencies from 2.54 up to 291 GHz. The weather conditions at IRAM 30-m were excellent during five days of observations (zenith opacity at 225 GHz < 0.25), contributing to the successful detections at the highest frequencies. In addition, the magnetar was particularly bright in the millimetre band during this observing campaign, with a varying flux density of mean value (averaged over all the millimetre observations) $\langle S_{\text{mm}} \rangle = 5.5 \pm 0.4$ mJy. This is a factor ~ 4 brighter than in July 2014 (Torre et al. 2015). In contrast, at the lowest frequencies, 2.54 to 8.35 GHz, the magnetar was a factor ~ 6 dimmer than in July 2014.

Figure 1 shows the averaged pulse profiles of SGR J1745–2900 at all frequencies from 2.54 to 291 GHz. The detections at 209 and 225 GHz are now clear with peak signal-to-noise ratios of about 12, confirming the tentative detections presented in Torre et al. (2015). At the highest frequencies, 275 and 291 GHz, the detections are weaker, but the alignment of the peaks with the pulse arrival phase predicted by the timing ephemeris and the simultaneous detections at other frequencies strengthen their significance. To verify that the pulses at 275 and 291 GHz were not an artefact of the on-pulse window protection in our cleaning method we carried out several tests. First, we applied the same cleaning shifting the protection window by 0.25 in rotational phase, and confirmed that no peak was artificially produced. Secondly, we applied the cleaning method without the on-pulse window protection, obtaining also peaks, although less significant. This is expected since the running mean tends to dip the pulse if not protected. We produced a periodogram of the significance of the profiles at 275 and 291 GHz without protecting the on-pulse window, folding the data at the spin frequency of the magnetar, and at nearby frequencies. The periodogram shows that the significant pulses are present only when folding at exactly the correct spin frequency (see Fig. 2).

Table 2 presents the measured mean flux densities and spectral index per day, together with the total averaged values. The high system temperatures and red noise (dominated by atmospheric effects) at 275 and 291 GHz made the detections at these frequencies challenging on individual days. Once the observations were combined, we obtained more significant detections (see Fig. 1) and measurements of the mean flux densities.

We remark that the flux density values presented in Table 2 for each frequency are averages per day. In some cases, the intensity of SGR J1745–2900 varied between different single observations by up to a factor of 2, in less than a few hours. Furthermore, within single observations, the flux density is sometimes seen to vary by a factor of a few in what seems to be a bursty behaviour. We investigated if

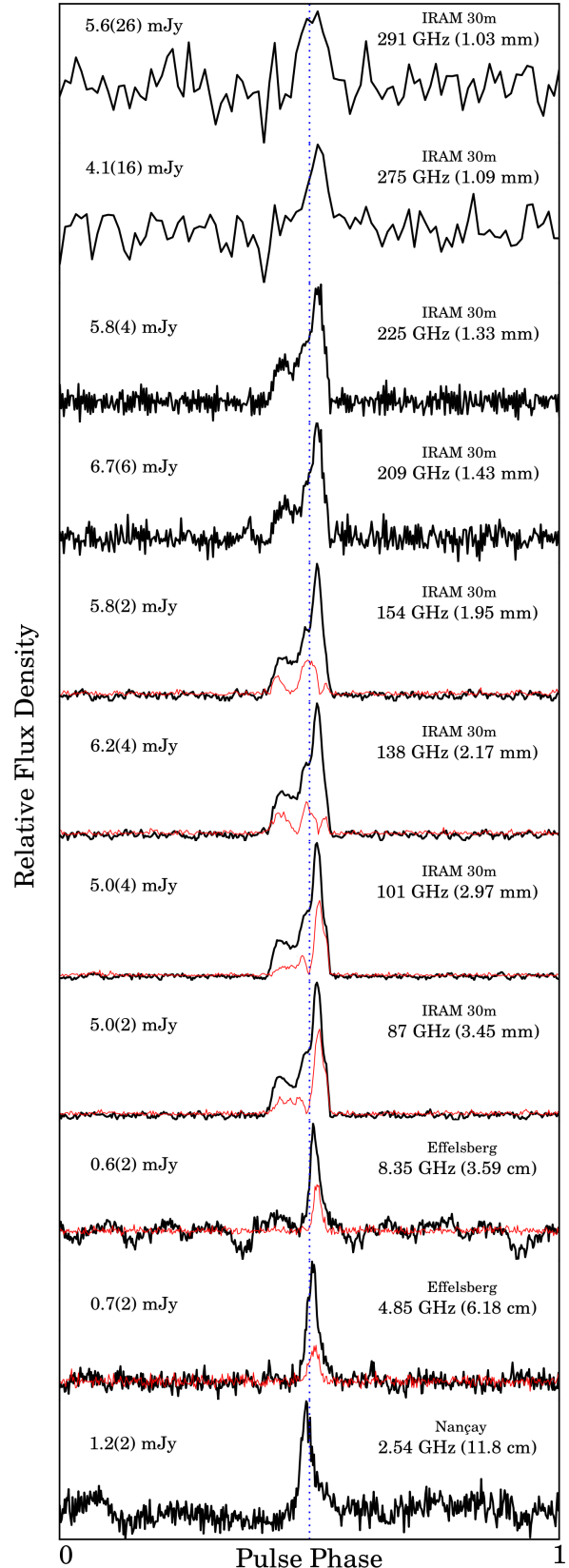


Figure 1. Average profiles of SGR J1745–2900 from 2.54 up to 291 GHz. The black thick line represents the total intensity profile, and the red thinner line shows the linear polarization, which is a lower limit between 87 and 154 GHz (see text). The vertical dotted line marks the predicted rotational phase from the ephemeris.

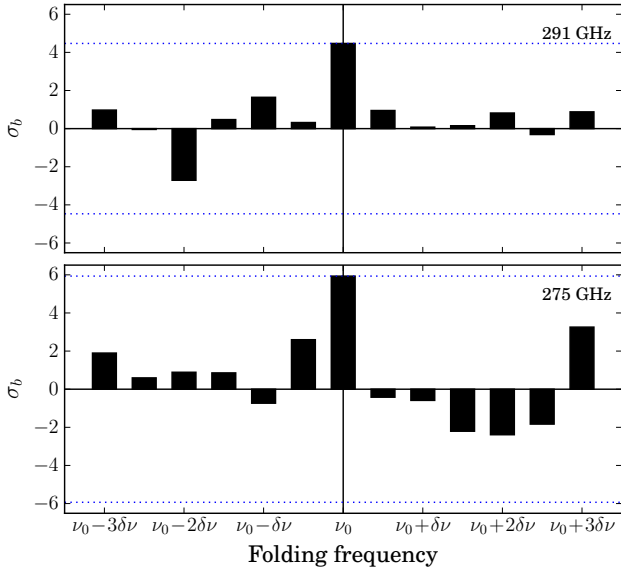


Figure 2. Periodogram of the significance of the profiles at 275 and 291 GHz when applying the cleaning method without protecting the on-pulse window from the running mean. The significance figure is calculated by adding the intensity over the on-pulse window and dividing by the standard deviation of the off-pulse region: $\sigma_b = \sum I[\text{on}] / \sqrt{\sum (I[\text{off}] - \mu)^2 / N}$, where μ and N are, respectively, the mean and the number of bins in the off-pulse region. The folding frequency is shifted in steps of half a Fourier bin of the longest individual integration length (45 min), i.e. $\delta\nu = 0.370$ mHz. Each step therefore corresponds to a variation of the folding frequency of ≈ 0.07 per cent. σ_b reaches values of 5.9 and 4.5, for 275 and 291 GHz, respectively; values that increase to $\sigma_b = 18.5$ and 10.6, respectively, when the pulse is protected from the running mean as described in Section 2.

the scintillation effect in the ISM could be responsible for this variability. Following Cordes & Lazio (1991), we calculate that the scintillation at the lowest frequencies, 2.54, 4.85 and 8.35 GHz, is negligible (and so, the variability of the magnetar at these frequencies must be intrinsic). At the millimetre wavelengths (87 GHz and above) the scintillation cannot be fully neglected, but at most it could account for an intensity modulation of a few tens of per cent. This could explain small intensity variations between consecutive days (see Table 2), as the refractive interstellar scintillation can have time scales down to a few days, but it cannot account for the variations of factors of a few that we also observe. Therefore, at the millimetre wavelengths the emission of SGR J1745–2900 must also have a large fraction of intrinsic variability. Furthermore, the variations of SGR J1745–2900 are not only in radio flux density and spectral index, but also in profile shape and polarization characteristics, a behaviour similar to what has been reported for this and the other known radio magnetars (e.g. Kramer et al. 2007; Camilo et al. 2007a, 2008; Levin et al. 2012; Lynch et al. 2015; Pennucci et al. 2015).

Figure 3 shows the observed averaged spectrum of SGR J1745–2900. Interestingly, the magnetar was clearly weaker at the lower frequencies, 2.54 to 8.35 GHz. A single power law fit yields a slightly inverted spectral index of

$\langle\alpha\rangle = +0.4 \pm 0.2$. This is still consistent with a flat spectrum typical from radio loud magnetars, but it is somewhat different to the spectrum observed for the same source in July 2014 ($\langle\alpha\rangle = -0.4 \pm 0.2$; Torne et al. 2015).

It is noticeable that the single power law does not fit well all the data points (in particular 4.85 and 8.35 GHz). We can think of several possible explanations. The first is that the intrinsic variability of the source behaves differently at different frequencies and deviates the spectrum from the single power law. A second possibility is that the measurements at low frequencies suffer from some systematic error, perhaps due to interference or red noise. The detections at Effelsberg were weaker than in the previous observing campaign in July 2014 (Torne et al. 2015) and the profile baseline showed some non-Gaussian noise (see e.g. the 8.35 GHz averaged profile in Fig. 1), which could lead to an under or overestimation of the flux density if the pulse lies on a dip or bump of the baseline, respectively. However, such effects would not account for deviations in the measurements larger than a few tens of per cent and are reflected in the errors at those frequencies. Thus, we consider this explanation less likely. Finally, a last possible explanation could be that there is a turn-up in the spectrum somewhere between 8.35 and 87 GHz. A turn-up might occur as a result of the decrease in the efficiency of the coherent radiation mechanism, together with an incoherent component of emission that could take over. This effect is predicted by some pulsar emission models (Michel 1978, 1982), and hints of turn-ups have in fact been observed in some pulsars at around ~ 30 GHz (Wielebinski et al. 1993; Kramer et al. 1996, 1997). Moreover, an incompatibility with a single power law has also been reported for the spectrum of another radio magnetar, 1E 1547.0–5408 (Camilo et al. 2008), suggesting the possibility of more complex spectra in radio magnetars than the typical single or broken power law of normal pulsars. The location of the possible turn-up in pulsar emission is not clear (it could be somewhere between radio and infrared, see Michel 1982), and SGR J1745–2900 is at the moment the only pulsar detectable from a few up to a few hundreds of gigahertz, which could be key to detect that possible turn-up in its spectrum. Additional simultaneous multifrequency observations covering the region around ~ 30 –40 GHz would be helpful to solve the turn-up question.

3.2 Linear polarization

Apart from the total intensity detections, we observe evidence of linear polarization in the emission from SGR J1745–2900, including at the millimetre wavelengths. This is obvious from the comparison of the pulse profile morphology from the horizontal (H) and vertical (V) linear feeds of the IRAM 30-m, which clearly show a different profile shape in most of the observations. Figure 4 shows a comparison of the H and V pulse profiles at 87, 101 and 154 GHz as an example.

This pulse profile morphology inequality when recording data with orthogonal linear feeds is indicative of radiation that must have a certain degree of linear polarization. Unfortunately, the BBC backend does not provide all Stokes parameters, making it not possible to quantify the degree of both linear and circular polarization in the millimetre emission directly. However, we can calculate Stokes Q from the power of the two linear feeds and set a lower limit in the

Table 1. Summary of the observations. For each day and frequency (ν), the total integration time ($T_{\text{obs},\nu}$) on SGR J1745–2900 is given in minutes. The symbol “–” means that no observation was done at that frequency on that particular day. The observations at 2.54 GHz were taken with Nançay, 4.85 and 8.35 GHz with Effelsberg, and 87 to 291 GHz with IRAM 30-m.

Date	$T_{\text{obs}2.54}$ (min)	$T_{\text{obs}4.85}$ (min)	$T_{\text{obs}8.35}$ (min)	$T_{\text{obs}87}$ (min)	$T_{\text{obs}101}$ (min)	$T_{\text{obs}138}$ (min)	$T_{\text{obs}154}$ (min)	$T_{\text{obs}209}$ (min)	$T_{\text{obs}225}$ (min)	$T_{\text{obs}275}$ (min)	$T_{\text{obs}291}$ (min)	MJD (days)
2015 Mar 04	55	72	72	180	180	90	90	90	90	–	–	57085
2015 Mar 05	–	–	–	90	90	90	90	90	90	90	90	57086
2015 Mar 06	–	60	60	90	90	90	90	90	90	90	90	57087
2015 Mar 07	72	–	–	78	78	45	45	78	78	45	45	57088
2015 Mar 08	–	66	72	90	90	185	185	–	–	95	95	57089
2015 Mar 09	72	–	–	45	45	45	45	–	–	–	–	57090

Table 2. Measured flux densities and spectral indices of SGR J1745–2900. Two-sigma errors in the last digits are shown in parentheses. The symbol “–” means that no observation was done at that frequency on that particular day. “ND” indicates observations with no detection.

Date (2015)	$S_{2.54}$ (mJy)	$S_{4.85}$ (mJy)	$S_{8.35}$ (mJy)	S_{87} (mJy)	S_{101} (mJy)	S_{138} (mJy)	S_{154} (mJy)	S_{209} (mJy)	S_{225} (mJy)	S_{275} (mJy)	S_{291} (mJy)	α
2015 Mar 04	1.0(2)	0.9(2)	0.8(2)	6.2(2)	6.4(2)	7.7(2)	6.3(4)	5.9(14)	3.7(8)	–	–	+0.5(4)
2015 Mar 05	–	–	–	5.4(2)	5.0(2)	6.3(2)	5.3(2)	6.9(8)	7.0(6)	4.6(28)	4.5(38)	+0.2(6)
2015 Mar 06	–	0.7(2)	0.6(2)	3.7(2)	3.7(2)	7.5(2)	6.5(2)	5.5(10)	5.1(8)	5.9(24)	6.7(36)	+0.8(6)
2015 Mar 07	1.4(6)	–	–	6.4(2)	5.7(2)	6.4(2)	5.8(2)	8.5(12)	7.2(6)	ND	ND	+0.1(6)
2015 Mar 08	–	0.4(2)	0.4(2)	5.1(2)	5.1(2)	5.3(2)	5.9(2)	–	–	1.6(30)	ND	+0.4(6)
2015 Mar 09	1.2(2)	–	–	3.4(2)	4.3(4)	3.8(6)	4.7(6)	–	–	–	–	+0.3(2)
Total Average	1.2(2)	0.7(2)	0.6(2)	5.0(2)	5.0(4)	6.2(4)	5.8(2)	6.7(6)	5.8(4)	4.1(16)	5.6(26)	+0.4(2)

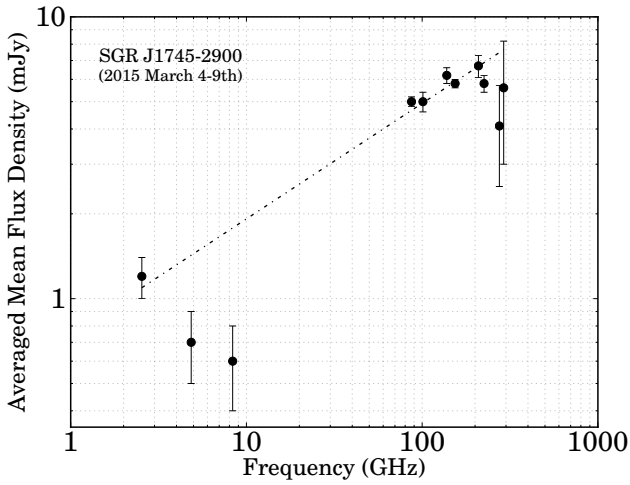


Figure 3. Average spectrum of SGR J1745–2900 from the observations. The dashed-dotted line shows the spectral index fit using a single power law. The mean spectral index obtained is $\langle\alpha\rangle = +0.4 \pm 0.2$. Error bars are 2σ .

degree of linear polarization: $L = \sqrt{Q^2 + U^2} \geq |Q|$. The lower limit of L reaches values as high as 100 per cent for certain profile bins, and it is greater than zero for most of the pulse (see Fig. 4 and 1). Moreover, minimum values of L greater than zero are noticeable in certain profile bins up to 225 GHz, and tentatively at 275 GHz. At 291 GHz the detections are too weak to be conclusive. However, the noise levels are higher above 154 GHz, and we also note apparent correlated noise between the two polarizations for frequen-

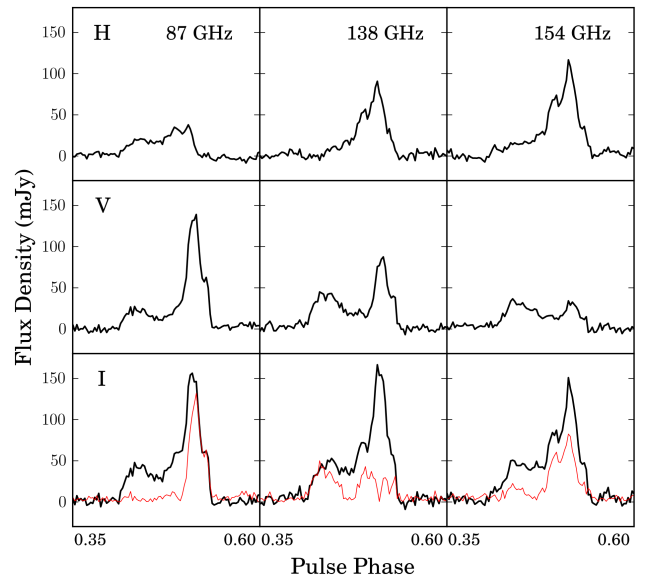


Figure 4. Selected examples of the pulse profile morphology differences seen in the two linear feeds of the IRAM 30-m at three different frequencies. The top panels show the profile detected on the horizontal feed (H), the middle panels on the vertical feed (V), and the bottom panels show the total intensity $I = H + V$ (black thick line), with the lower limit of the degree of linear polarization (red thin line, see text). The differences in the profile shape between the two feeds are recurrent, and the lower limit on the degree of linear polarization is greater than zero in many bins across the profile (see also Fig. 1), reaching values of up to 100 per cent linearly polarized emission for some profile bins.

cies between 209 and 291 GHz. The origin of this noise is not fully understood and, for this reason, we do not show here the lower limits on L for frequencies above 154 GHz. Ongoing work for a more detailed analysis of the polarized emission from SGR J1745–2900 will be presented in a future publication (Wucknitz et al. in prep.).

This is the first time linearly polarized emission up to 154 GHz (1.95 mm) has been seen in a pulsar. It is closely followed by XTE J1810–197, with inferred linear polarization up to 144 GHz (Camilo et al. 2007c). For normal pulsars, the highest radio frequency at which polarization has been detected is 32 GHz (Xilouris et al. 1996). Polarized emission at such high level and frequencies as seen for SGR J1745–2900 is unusual, as radio pulsars have been reported to depolarize at high radio frequencies (Morris et al. 1981; Xilouris et al. 1996). In contrast, radio magnetars can stay highly linearly polarized up to very high frequencies (Kramer et al. 2007; Camilo et al. 2008). Consequently, the polarized emission at millimetre wavelengths of SGR J1745–2900 is not totally unexpected. In fact, Kravchenko et al. (2016) measured an averaged linear polarization for this magnetar of about 65 per cent at ~ 40 GHz.

The polarization in pulsar emission is generally linked with a coherent radiation mechanism. The fact that high degrees of linear polarization are measured at the millimetre wavelengths for SGR J1745–2900 therefore may conflict and weaken the idea of an incoherent component of emission responsible for a turn-up in its spectrum.

4 SUMMARY

We show in this paper that the radio emission from highly magnetized neutron stars can reach extremely high frequencies with detections that reach 291 GHz (1.03 mm). These new detections break the previous record recently set in Torne et al. (2015) as the highest radio frequency detection of pulsar emission, and give us more hints about the radiation mechanism of these objects. SGR J1745–2900 continues to show significant variability in its emission characteristics, and its averaged mean flux density in the millimetre band is a factor ~ 4 higher than in July 2014, while between 2.54 and 8.35 GHz is on average a factor ~ 6 dimmer. Furthermore, we show evidence for a significant degree of linear polarization in the millimetre emission from SGR J1745–2900, reaching factors up to a 100 per cent for certain profile bins, and being the polarized emission at the highest radio frequencies ever detected from a pulsar. The measured spectrum is slightly inverted, with a spectral index of $\langle\alpha\rangle = +0.4 \pm 0.2$ when a single power law is fit. The spectrum has an uncommon shape, with decaying flux density between 2.54 and 8.35 GHz and a much stronger emission at the millimetre band, which may be due to intrinsic intensity variability or indicative of the existence of a turn-up in the emission somewhere between 8.35 and 87 GHz. These new results are relevant to the development of better pulsar emission models, in particular those trying to explain the radio emission from magnetars; and are also further proof that we can detect and study pulsars located at the Galactic Centre using millimetre wavelengths.

ACKNOWLEDGEMENTS

We thank the anonymous referee for a careful review and constructive comments that helped improving the manuscript. We also thank Olaf Wucknitz and Dominic Schnitzler for discussions on the polarization analysis, Jim Cordes for discussions on scintillation effects, and the staff at the IRAM 30-m for their great support. Based on observations carried out with the IRAM 30-m, the Effelsberg 100-m, and the Nançay radio telescopes. The Nançay radio observatory is operated by the Paris Observatory, associated to the French CNRS. The Effelsberg 100-m is operated by the MPIfR (Max-Planck-Institut für Radioastronomie). IRAM is supported by INSU/CNRS (France), MPG (Germany) and IGN (Spain). P.T. is supported for this research through a stipend from the International Max Planck Research School (IMPRS). Financial support by the European Research Council for the ERC Synergy Grant *BlackHoleCam* (ERC-2013-SyG, Grant Agreement no. 610058) is gratefully acknowledged. L.G.S. gratefully acknowledges financial support from the ERC Starting Grant BEACON under contract no. 279702.

REFERENCES

- Bower G. C., et al., 2014, *ApJ*, **780**, L2
 Bower G. C., et al., 2015, *ApJ*, **798**, L20
 Camilo F., Ransom S. M., Halpern J. P., Reynolds J., Helfand D. J., Zimmerman N., Sarkissian J., 2006, *Nature*, **442**, 892
 Camilo F., et al., 2007a, *ApJ*, **663**, 497
 Camilo F., Ransom S. M., Halpern J. P., Reynolds J., 2007b, *ApJ*, **666**, L93
 Camilo F., et al., 2007c, *ApJ*, **669**, 561
 Camilo F., Reynolds J., Johnston S., Halpern J. P., Ransom S. M., 2008, *ApJ*, **679**, 681
 Carter M., et al., 2012, *A&A*, **538**, A89
 Cordes J. M., Lazio T. J., 1991, *ApJ*, **376**, L23
 Duncan R. C., Thompson C., 1992, *ApJ*, **392**, L9
 Eatough R. P., et al., 2013, *Nature*, **501**, 391
 Hankins T. H., Rankin J. M., Eilek J. A., 2009, in *astro2010: The Astronomy and Astrophysics Decadal Survey*.
 Kramer C., 1997, Technical report, Calibration of spectral line data at the IRAM 30m radio telescope. IRAM
 Kramer M., Xilouris K. M., Jessner A., Wielebinski R., Timofeev M., 1996, *A&A*, **306**, 867
 Kramer M., Jessner A., Doroshenko O., Wielebinski R., 1997, *ApJ*, **488**, 364
 Kramer M., Stappers B. W., Jessner A., Lyne A. G., Jordan C. A., 2007, *MNRAS*, **377**, 107
 Kravchenko E. V., Cotton W. D., Yusef-Zadeh F., Kovalev Y. Y., 2016, *MNRAS*, **458**, 4456
 Lazaridis K., Jessner A., Kramer M., Stappers B. W., Lyne A. G., Jordan C. A., Serylak M., Zensus J. A., 2008, *MNRAS*, **390**, 839
 Levin L., et al., 2010, *ApJ*, **721**, L33
 Levin L., et al., 2012, *MNRAS*, **422**, 2489
 Löhmer O., Jessner A., Kramer M., Wielebinski R., Maron O., 2008, *A&A*, **480**, 623
 Lynch R. S., Archibald R. F., Kaspi V. M., Scholz P., 2015, *ApJ*, **806**, 266
 Maron O., Kijak J., Kramer M., Wielebinski R., 2000, *A&AS*, **147**, 195
 Melrose D. B., Yuen R., 2016, *Journal of Plasma Physics*, **82**, 635820202
 Michel F. C., 1978, *ApJ*, **220**, 1101

- Michel F. C., 1982, *Reviews of Modern Physics*, **54**, 1
- Morris D., Graham D. A., Sieber W., Bartel N., Thomasson P., 1981, *A&AS*, **46**, 421
- Morris D., et al., 1997, *A&A*, **322**, L17
- Olausen S. A., Kaspi V. M., 2014, *ApJS*, **212**, 6
- Peñalver J., 2012, Technical report, Antenna Technical Works. IRAM
- Pennucci T. T., et al., 2015, *ApJ*, **808**, 81
- Shannon R. M., Johnston S., 2013, *MNRAS*, **435**, L29
- Spitler L. G., et al., 2014, *ApJ*, **780**, L3
- Thompson C., Duncan R. C., 1995, *MNRAS*, **275**, 255
- Thompson C., Duncan R. C., 1996, *ApJ*, **473**, 322
- Torne P., et al., 2015, *MNRAS*, **451**, L50
- Wielebinski R., Jessner A., Kramer M., Gil J. A., 1993, *A&A*, **272**, L13
- Xilouris K. M., Kramer M., Jessner A., Wielebinski R., Timofeev M., 1996, *A&A*, **309**, 481

This paper has been typeset from a $\text{\TeX}/\text{\LaTeX}$ file prepared by the author.